ENTRY DEBRIS FIELD ESTIMATION METHODS AND APPLICATION TO COMPTON GAMMA RAY OBSERVATORY DISPOSAL

Richard B. Mrozinski
Flight Design and Dynamics Division
Mission Operations Directorate
NASA Johnson Space Center

ABSTRACT

For public safety reasons, the Compton Gamma Ray Observatory (CGRO) was intentionally deorbited on June 04, 2000. This deorbit was NASA's first intentional controlled deorbit of a satellite, and more will come including the eventual deorbit of the International Space Station. To maximize public safety, satellite deorbit planning requires conservative estimates of the debris footprint size and location. These estimates are needed to properly design a deorbit sequence that places the debris footprint over unpopulated areas, including protection for deorbit contingencies.

This paper details a method for estimating the length (range), width (crossrange), and location of entry and breakup debris footprints. This method utilizes a three degree-of-freedom Monte Carlo simulation incorporating uncertainties in all aspects of the problem, including vehicle and environment uncertainties. The method incorporates a range of debris characteristics based on historical data in addition to any vehicle-specific debris catalog information. This paper describes the method in detail, and presents results of its application as used in planning the deorbit of the CGRO.

BACKGROUND

NASA launched the CGRO aboard the Space Shuttle on April 5, 1991 to study gamma-ray phenomena. It surpassed its lifetime goal of 5 years and continued operating without any mission-threatening failures until one of the three gyroscopes failed on December 6, 1999. This failure placed the spacecraft within one additional gyro failure of potentially losing the capability for a controlled entry. The risk of a public death or serious injury due to an uncontrolled entry from its 28.5° inclination was an estimated 1/1000. As a result, the design of the spacecraft included as its end-of-life disposal the ability to target the entry and resulting debris field for an ocean impact. The much-improved risk associated with a controlled entry was an estimated 1/29,000,000. After considering a wide range of options, NASA decided to reenter CGRO in June 2000, while the two remaining gyros could allow a controlled entry, to minimize risks to public safety*.

Although footprint analyses for CGRO were presented by TRW (ref. 1) and some results were also shown by NASA's Goddard Space Flight Center (GSFC) (ref. 2) prior to launch, this document presents an alternate method used at NASA's Johnson Space Center (JSC) to estimate the size and location of the debris footprint resulting from the entry and breakup of the CGRO. GSFC used this footprint data as verification of previous results in computing entry opportunities that best ensured public safety, placing the debris footprint entirely over water as required. The actual entry of the vehicle did in fact result in water disposal in the planned target area.

SYMBOLS AND UNITS

Values in this paper are presented in standard SI units, with English Engineering System units provided in parentheses following the SI values. All calculations were done in English Engineering System units. Symbols used are as follows:

C_d	Effective average drag coefficient (eq. 1)
C_l	Effective average lift coefficient
L/D	Effective average lift-to-drag ratio, C_l/C_d
m	Effective average mass (eq. 1)

* "CGRO Reentry, Independent Engineering Review, Operations Readiness Review," presentation, NASA Goddard Space Flight Center, Greenbelt, Maryland, May 4-5, 2000.

S Reference aerodynamic surface area (eq. 1)
β Effective average ballistic coefficient, $m/S \cdot C_d$ (eq. 1)
ϕ Bank angle
σ One standard deviation of sample output data

METHOD OVERVIEW

A three degree-of-freedom simulation was built using version 8.0 of the Simulation and Optimization of Rocket Trajectories (ref. 3) (SORT) program at JSC. The simulation was built assuming an instantaneous breakup of the CGRO vehicle at a given altitude, not a multiple-stage breakup over an altitude region. The intact CGRO vehicle was modeled as a point mass (constant orientation), with aerodynamic and mass properties held constant. The assumption of constant mass was acceptable because there are no significant mass or shape changes prior to breakup. The assumption of constant aerodynamics was also valid, as the aerodynamic coefficients used in this study were intended to represent equivalent average values. Additionally, it has been shown that the regime in which drag coefficient changes significantly occurs after the debris achieves vertical flight, and therefore has no impact on footprint size (ref. 4). The constant orientation assumption has no impact since no lift was modeled prior to breakup.

Beginning at the breakup altitude, the simulation then modeled a single debris piece down to an altitude of 15.24 km (50,000 ft), which was considered as ground impact. At the breakup altitude, an instantaneous change in mass, aerodynamics, and bank angle were modeled, all of which were then held constant to ground impact. Holding the bank angle constant was not overly conservative because a reduced lift-to-drag ratio was used which assumed a constant bank orientation[†]. The assumption of constant mass and aerodynamics was erroneous in reality due to the ablation of debris pieces through their entry. However, in modeling the debris here, the ballistic coefficients used were intended to represent equivalent average values, rather than the actual indeterminable values.

Although a hydrazine explosion was a possible breakup situation, it was not accounted for here for two reasons. First, any explosion would have been nearly impossible to model with any certainty without performing a detailed blast analysis. Second, regardless of any answers that such an analysis would have produced, the most that could be done to protect for public safety was done by GSFC by placing the footprint in the middle of the available ocean area as much as possible.

Using nominal vehicle properties and assuming no breakup, an intact reference trajectory and corresponding impact point for the intact vehicle were determined. This point was not very realistic, as a breakup was guaranteed, but provided a good reference point. Monte Carlo methods were also needed to account for all non-linearities and the large number of variables involved. This method used the 1995 Global Reference Atmosphere Model (GRAM-95) and localized winds. The Monte Carlo runs included variations in: drag coefficient, lift coefficient, reference aerodynamic surface area, and mass for both the intact vehicle before breakup and the debris pieces after vehicle breakup, for several initial conditions provided by GSFC. All variations were distributed in a uniform distribution, to be most conservative. Two thousand cases were run (see "Evaluation of Number of Monte Carlo Cases Required and Associated Errors"), producing two thousand impact points.

MODELS AND ASSUMPTIONS

Here, various models are described as well as the assumptions involved. Since the footprint was planned for an open ocean area, the analysis was conservative wherever possible and reasonable.

Integration Method

A fourth-order Runge-Kutta method was used to integrate the equations of motion. An integration step size of one second was used throughout the trajectory, except for five seconds beginning at breakup where the step size was reduced to 0.01 second. This reduction was used to allow the dynamics to adjust to instantaneous changes in mass and aerodynamics. Integration method effects on the footprint were assumed minimal, and were not investigated further.

† Cerimele, C. J., conversation, NASA Johnson Space Center, Houston, Texas, May 03, 2000.

Planet and Gravity Models

The planet model used in this study was an oblate spheroid planet, set by the equatorial and polar radii (ref 3). The polar axis was considered an axial axis of symmetry, and was assumed to be the planet's rotational axis. The gravitational model consisted of the central gravitational force adjusted via the first three oblate zonal harmonic coefficients (J_2, J_3, and J_4) (ref 3). Planet and gravity model variations were assumed to have minimal effect on the resulting footprint, and were not investigated further.

Atmosphere Model

Experience with the methods used here has shown that winds have significant impact on the width of the footprint (more pronounced near the heel, or lowest range part of the footprint), but negligible impact on the footprint's length characteristics cases[‡]. Thus, our Monte Carlo method used the GRAM-95 atmosphere model and wind database, which also models density variations and shears. Note that the density variations and shears, as well as the winds produced by the GRAM model were localized. That is, the density perturbations and winds were specific to the latitudinal and longitudinal position, as well as altitude, month, etc. Here, GRAM was used assuming an entry date of June 04, 2000.

Guidance, Navigation, and Control

The guidance, navigation, and control (GN&C) system was disabled, as the vehicle would be in a completely uncontrolled trajectory. The attitude of the CGRO vehicle was forced to be constant relative to a Local-Vertical/Local-Horizontal, as discussed in "Method Overview".

Aerodynamics and Mass Properties

Ideally, we would input into the simulation only the ballistic coefficient (β) and lift-to-drag ratio (L/D). However, SORT requires mass properties for simulation, therefore we had to provide each component of the ballistic coefficient: drag coefficient (C_d), reference aerodynamic surface area (S), and mass (m). Note that designating values of these latter three variables was arbitrary, since when the lift is zero it is only the ballistic coefficient that dictates the trajectory of the vehicle or debris. See Equation 1.

$$\beta = m/(S \cdot Cd) \tag{1}$$

We now discuss the aerodynamic and mass properties used in this study beginning with the properties of the intact (pre-breakup) CGRO. We will then move to the post-breakup debris properties.

Intact CGRO Characteristics

The wet mass of the CGRO spacecraft was 14910.0 kg (32870.8842 lb)[*] at the time of this study. To arrive at the entry mass, we deducted the amount of expected fuel used in the deorbit maneuvers. The fuel usage estimated for the four deorbit burns was 238.74, 218.57, 201.96, and 240.78 kg (526.32, 481.85, 445.2428, and 530.8112 lb)[*], for burns 1, 2, 3, and 4 respectively, for a total of 900.04 kg (1984.2240 lb), where the uncertainty in mass during entry was conservatively estimated as 10% of the remaining fuel mass, which was 366.1 kg (807.0 lb) worst case (cold burns)[§]. Thus, we arrived at an entry mass of 14010.0 ± 36.6 kg (30886.6602 ± 80.7 lb). The mass for the intact (reference) case was taken as the midpoint of this range.

For intact aerodynamics, we began with the aerodynamic cross-sectional surface area of 46.0 m^2 (495.14 ft^2) (ref 2). A drag coefficient (C_d) of 2.2 was used in References 2 and §. An analysis of CGRO surviving debris showed a range of 0.91 - 2.05 for the intact vehicle drag coefficient (ref. 5). To bound all cases, we selected a range of 0.91 - 2.20. The drag coefficient for the intact (reference) case was taken as the midpoint of this range (1.555). Combining these assumptions to arrive at maximum and minimum ballistic coefficients, we found the extremes in mass and drag led to a ballistic coefficient range for the

‡ Mrozinski, R. B., "CRV Deorbit Opportunities, v1.0h," unpublished, NASA Johnson Space Center, Houston, Texas, January 24, 2000.

§ Vaughn, F., "RE: Vectors for Rich," e-mail communication, NASA Goddard Space Flight Center, Greenbelt, Maryland, May 18, 2000.

intact CGRO of 138.8 - 335.4 kg/m^2 (28.3 - 68.7 psf). This range covered values seen in previous reports of 175.8, 139.6, and 273.4 kg/m^2 (36.0, 28.6, and 56.0 psf) in References 1, 2, and * respectively. Although tumbling was not planned to be explicitly induced as the CGRO entered the atmosphere, GSFC predicted that the intact CGRO vehicle would begin a random tumble on its own*. Due to this prediction, and previous work showing that L/D prior to breakup has negligible impact on debris footprints for objects that break up above 74 km (40 nmi)‡, we set the intact L/D to zero in all cases.

The intact (reference) intact mass and aerodynamic properties are summarized in Table 1. Note that in determining this reference impact point, it was assumed that no vehicle breakup occurs. The Monte Carlo input data is given in Table 2.

Post-Breakup Debris Characteristics

It was impossible to say with any certainty exactly what the majority of the CGRO debris pieces would look like and what characteristics they would have. Therefore, we arrived at assumptions for the generic debris ballistic and lift coefficients by surveying previous disposal analyses for historical data. Once settling on a range of general debris characteristics, we examined an analysis that was done that predicted some particular debris pieces that were likely to survive. Some of these pieces were outside the historical range we selected; therefore separate studies were done focusing on just the most extreme of these unique pieces.

Some ballistic coefficient ranges used in previous studies for various vehicles are shown in Table 3. A range of 2.4 - 659.1 kg/m^2 (0.5 - 135 psf) was used in previous CGRO entry studies (ref. 1, 2). After discussions with one of the original authors (McCormick) of the source of the Skylab data, it was concluded that the maximum ballistic coefficient of 1562.4 kg/m^2 (320 psf) used in Skylab analyses is much too high for typical vehicles, as this value corresponded to an aluminum film safe onboard Skylab, and values of no greater than 683.5 kg/m^2 (140 psf) should be used.** Thus, the 1562.4 kg/m^2 (320 psf) value was excluded. The low end was felt to be adequately conservative at 2.4 kg/m^2 (0.5 psf) since pieces of less than this value have the lowest capability of all the pieces to cause damage. Thus, for the general debris field, we adopted the prior CGRO study range of 2.4 - 659.1 kg/m^2 (0.5 - 135 psf), which encompasses all other historical data that could be found.

Given this range of ballistic coefficients, we had to then select appropriate values of mass, drag coefficient, and aerodynamic surface area which produced the limits of this range. The values that were selected were arbitrary, as long as the resulting ballistic coefficients were correct. For all debris pieces, we selected a drag coefficient of 1.0, and a mass of 22.7 kg (50.0 lb). Thus, by choosing a surface area range of 0.0344 - 9.29 m^2 (0.3704 ft^2 - 100.0 ft^2) we arrived at the desired ballistic coefficient range.

Next, we had to select a range of lift-to-drag ratios. A maximum ratio of 0.15 was found in studies done for the Soyuz launch vehicle (ref. 6). Although debris pieces could exhibit higher L/D values, they were unlikely to hold the lift vector in a constant orientation as we were modeling here. The 0.15 value is a reduced L/D that applies when constant bank angles are used†. Since we assumed that the pieces of debris would neither trim at a stable orientation, nor tumble at a high enough rate to generate substantial lift, we were safely able to assume a lift-to-drag ratio in the range of 0.0 - 0.15. Bank angle is allowed to vary from 0.0 – 360.0 degrees.

The resulting Monte Carlo data for the general debris field is summarized in Table 4.

We now discuss the case of defined debris pieces that we had to consider separately. An analysis of CGRO surviving debris predicted a piece of one of CGRO's science instruments would survive with a ballistic coefficient ranging from approximately 1200 - 1260 kg/m^2 (246 - 259 psf); this piece was the Total Absorption Shower Counter (TASC) component within the Energetic Gamma Ray Experiment Telescope (EGRET) science instrument (ref 5). The TASC was not the only piece with a ballistic coefficient above 659.1 kg/m^2 (135 psf), but it was the maximum, and would clearly extend the footprint length beyond the historical-based footprint and redefine the highest range end (toe) of the footprint. To account for this, we ran separate Monte Carlo runs where the debris characteristics were limited to this piece. We again set the mass and aerodynamic properties rather arbitrarily to arrive at the desired range of ballistic coefficients of 1200 - 1260 kg/m^2 (246 - 259 psf). We set drag coefficient to 1.44 and mass to 528.6 kg (1165.25 lb) (the average values of these two parameters seen in Reference 5). The aerodynamic reference area range that led to the desired ballistic coefficient range was then 0.29 - 0.31 m^2 (3.1243 - 3.2894 ft^2). To be conservative, we kept an L/D range of 0.0 - 0.15.

Reference 5 indicated no surviving debris pieces with a lower ballistic coefficient than our lower limit of 2.4 kg/m^2 (0.5 psf). However, we had to investigate the solar arrays as a piece whose ballistic coefficient was above this value, but was capable of redefining the heel of the footprint. This was possible because the arrays were very likely to separate from the intact CGRO vehicle at a higher altitude (100 km or 54 nmi) than the assumed breakup altitude (83.8 km or 45.2 nmi, see "Breakup Model"), which could allow the arrays to fly less range than all other pieces. We began by assuming a ballistic coefficient

** McCormick, P. O., e-mail communications, Lockheed Martin, January 2000.

range of 9.8 - 19.5 kg/m^2 (2.0 - 4.0 psf) for a single solar array. We then chose arbitrary values of drag coefficient and mass of 1.0 and 90.7 kg (200 lb) respectively. By choosing the aerodynamic reference area range of 4.7 - 9.3 m^2 (50.0 - 100.0 ft^2), we arrived at the desired ballistic coefficient range. To be conservative, we kept an L/D range of 0.0 - 0.15.

We eventually showed via parametric runs that the solar arrays breaking off at a higher altitude than the general breakup would not extend the footprint beyond that computed by using the historical range of general debris data dispersed from the nominal breakup altitude. This ended the solar array analysis; no solar array Monte Carlo simulations were run.

The resulting Monte Carlo data for the TASC debris field is summarized in Table 5.

Initial State

GSFC provided four pairs of state vectors on May 18, 2000, for each of the two primary disposal target areas in the South Pacific Ocean[††]. The prime disposal area is referred to here as the "center pass," and the backup area as the "western pass." For each disposal area, GSFC delivered the nominal burn 4 ignition and cutoff vector pair, as well as three other pairs corresponding to 10% hot, 10% cold, and 10% cold plus 12 minute late burn 4 scenarios. This wide variation in burn dispersions was assumed to be of much larger magnitude than all other possible uncertainties in the initial state, so the eight burn 4 cutoff vectors were used with no uncertainties added.

Termination Conditions

All simulations (reference intact and Monte Carlo) were terminated at an altitude of 15.24 km (50,000 ft). This was also done in the original TRW footprint analysis, where it was shown that errors on the order of 0.1 degree in latitude and longitude result by stopping at 50 km (164,000 ft) rather than 1 km (3280 ft) (ref 1). Regardless, we terminated at 15.24 km (50,000 ft), which we determined to be approximately the lowest the simulation can go on heel debris pieces without encountering chaotic wind impacts on heel pieces in near vertical flight. Additionally, the termination altitude of 15.24 km (50,000 ft) has been used in other footprint studies, such as for the Space Shuttle Super Lightweight External Tank (ref. 6).

Breakup Model

Breakup was assumed to occur at a single discrete altitude for modeling purposes. In reality breakup always occurs in multiple stages over an altitude range. Additionally, ablation can create a near-constant stream of new debris over a very large altitude range. It was impossible to predict or model the actual stages of breakup or when they will occur. Therefore, we modeled the entire breakup at an altitude high enough to be conservative (higher breakup altitudes generally lead to larger debris footprints). Entry tests show that typical satellites of aluminum or magnesium structure will breakup up around 77.8 km (42 nmi) (ref. 7). Results of breakup analyses' predictions and/or observations for various vehicles are shown in Table 6[‡‡] (ref. 6). Previous CGRO footprint analyses assumed a breakup at 83.8 km (45.25 nmi) (ref. 1, 2). Looking at the table and considering the typical value of 77.8 km (42 nmi), we saw the prior CGRO footprint estimate of 83.8 km (45.25 nmi) to be higher than the 77.8 km (42 nmi) typical value. Additionally, it is higher than all Table 6 values, except for the assumed values for the Super Lightweight tank and the 94.5 km (51 nmi) value for Skylab, which is extremely high. Therefore, we used the same breakup altitude as the previous CGRO studies, using 83.8 km (45.25 nmi), as this high value is conservative.

CGRO FOOTPRINT ESTIMATES

Here we first present some key results from a small parametric study, then results from the Monte Carlo study. All range values were calculated with respect to an arbitrary reference point. Here, we used the crossing of the orbit groundtrack (as determined by the initial conditions) with the west coast of South America. Thus, a range value of 2000 km indicates a location 2000 km west of South America along the orbit groundtrack. The reference points for the two passes are given in Table 7. The crossrange was calculated with respect to the initial orbital plane frozen at the vector time. A positive value indicates the debris landed to the right of the orbital groundtrack (in this case south of the groundtrack).

[††] "GRO Vectors," facsimile transmission, Guidance, Navigation, and Control Center, Code 570, NASA Goddard Space Flight Center, Greenbelt, Maryland, May 18, 2000.

[‡‡] Misc., "International Space Station Alpha (ISSA) End of Life Disposal Assessment," Aeroscience and Flight Mechanics Division, NASA Johnson Space Center, Houston, Texas, May 08, 1995.

Results of Parametric Study

A parametric study was used to investigate the need for separate Monte Carlo simulations for TASC and solar array debris. We saw a definite impact of the TASC debris piece, adding a predicted 400 km (216 nmi) to the footprint size. In other words, Monte Carlo studies were needed. We also saw that the solar arrays falling off 16.2 km (8.75 nmi) higher than the full breakup had no impact on footprint size, as it landed within the heel determined by using the historical general ballistic coefficient range data. Thus, solar array debris was not simulated individually in Monte Carlo simulations.

Results of Monte Carlo Studies

Monte Carlo simulations were run for the center pass only, for the hot, nominal, cold, and cold+late burn scenarios, as provided by GSFC (see "Initial State"). In each case, separate results were obtained for the general debris and the TASC debris. The western pass footprint was derived from the center pass analysis by applying the biases seen between the center and western pass in the parametric runs (see "Results of Parametric Study").

Results of the Monte Carlo study for the nominal deorbit burn 4 are shown in Table 8 for both the general and TASC debris footprints.

The width of the footprint was taken as the maximum of the general debris or the TASC debris results. The general debris should always have a larger width, because heel pieces have greater crossrange capability since they are in the air longer and are more sensitive to winds. We saw this to be the case here, and we found a width of 117.3 km (63.35 nmi).

In all cases, when taking the mean range value and extending it both ways by $\pm 3\sigma$ for both the general debris footprint and the TASC footprint, the two footprints did not overlap for any of the burn scenarios. Thus, to find the total footprint size for each burn, we subtracted the TASC footprint 3σ toe value from the general debris footprint 3σ heel value. See Equations 2 – 4 for the nominal burn as an example.

$$\text{Length} = (\text{General Debris } 3\sigma \text{ Heel Location}) - (\text{TASC Debris } 3\sigma \text{ Toe Location}) \quad (2)$$

$$\text{Length} = (5090.64 + 3*120.30) - (4306.13 - 3*93.00) \quad (3)$$

$$\text{Length} = 2638.01 \text{ km } (1424.41 \text{ nmi}) \quad (4)$$

The geometric center of the footprint for each burn scenario was calculated similarly, by averaging the TASC footprint 3σ toe value and the general debris footprint 3σ heel value. See Equations 5 – 7 for the nominal burn:

$$\text{Geometric Center} = [(\text{General Debris } 3\sigma \text{ Heel Location}) + (\text{TASC Debris } 3\sigma \text{ Toe Location})]/2 \quad (5)$$

$$\text{Geometric Center} = [(5090.64 + 3*120.30) + (4306.13 - 3*93.00)]/2 \quad (6)$$

$$\text{Geometric Center} = 8777.26 \text{ km } (4739.34 \text{ nmi}) \quad (7)$$

The center pass nominal burn Monte Carlo extreme 3σ impact points accounting for both the general and TASC debris are plotted along with the reference intact impact point in Figure 1.

Corresponding results for the center pass, 10% hot burn scenario are presented in Table 9 and Figure 2. Similarly, the results for the center pass, 10% cold/late burn scenario are presented in Table 10 and Figure 3.

Note that going from the hot burn scenario to the nominal burn, to the cold/late burn, the length and width of the footprint were steadily increasing. This was primarily due to shallower flight path angles at entry interface with colder burns.

Evaluation of Number of Monte Carlo Cases Required and Associated Errors

To ensure that by chance the initial set of seeds used throughout this study were not biasing the results, we ran another three sets, and compared the new results to the nominal burn results for the general debris field (not including the TASC footprint) in Table 8. We also studied the number of cases needed in a Monte Carlo run to achieve good estimates, and what magnitudes of errors were involved with a given set of 2000 trajectories in a Monte Carlo. This was all done by plotting in Figures 4 - 6 the running footprint length, width, and center (respectively) as each of the 2000 trajectories in the Monte Carlo runs were tabulated, up to 2000, for each of four separate Monte Carlo runs initiated with four different sets of initial seeds.

We saw from these figures that 2000 trajectories were more than enough for the statistics we were generating to settle down to a near-constant value. Inspecting the final values of each Monte Carlo run, we saw that by using the results of seed set #1 (as we did throughout), we may have had about an 148.2 km (80 nmi) error in length, less than 18.5 km (10 nmi) error in width, and 18.5 km (10 nmi) error in position of the geometric center.

Overall Footprint Estimates

Results of the Monte Carlo studies for the three burn scenarios for the center pass are summarized again in the top half of Table 11. The bottom half of this table shows the results when the three individual burn statistics were combined to achieve an overall footprint area to protect, as depicted in Figure 7. Note: the intact (reference) impact point ("INTACT") in this figure corresponds to the intact entry parametric case, not the geometric center of the footprint, which is labeled as "GEOMETRIC_CENTER".

No Monte Carlo cases were run for the Western Pass, only an intact reference impact trajectory. We approximated the corresponding extreme 3σ impact points by applying the same uprange/downrange deltas from the intact reference point as we saw for the Center Pass. Doing so provided a graphical estimate of the Western Pass footprint in Figure 8, and estimates of length and range position in Table 12 (note that crossrange position, length, and width do not change from the Center Pass, due to the approximation).

Footprint Proximity to Land Masses

Considering the proximity to the west coast of South America, we found that the closest a piece can come, with 3σ probability, was 4260 km (2300 nmi) in range (the toe of the TASC footprint for the cold/late burn) for the center pass, and 6465 km (3490 nmi) in range for the western pass.

After looking at various islands in the Pacific Ocean, we considered Figure 9 which plots the approximate centerlines for the overall footprint area to protect (covering all burn scenarios), for both the center and western pass (note that the center footprint extends beyond the right-hand-side of the page). To show the proximity to islands, we drew circles around those that were closest to the footprint of radius equal to half the footprint width (whole width was 67.5 km, or 36 nmi), plus either 46.3 km (25 nmi) if United States soil, or 370.4 km (200 nmi) if foreign soil. The 46.3 km (25 nmi) and 370.4 km (200 nmi) values are landmass miss distance guidelines suggested in NASA Safety Standard 1740.14 (ref. 8). By adding half the footprint width to the radius of these circles, the figures are interpreted as: the 3σ edge of the footprint was closer than the corresponding land-miss guideline (46.3 or 370.4 km) if the groundtrack went through a circle. Thus, we saw that the center pass footprint completely met NSS 1740 guidelines, while the western pass did not. However, for both passes, predictions showed that no island could hit by debris within a 3σ probability. For the center pass, the closest a piece could come to land, with 3σ probability, was 250 km (135 nmi) in crossrange to the Hawaiian Islands. For the western pass, the closest a piece could come to land, with 3σ probability, was 119 km (64 nmi) in crossrange to Palmyra Island. Other values are presented in Table 13.

CONCLUSIONS

This document presented results of Monte Carlo simulations of the CGRO entry, assuming breakup at 83.8 km (45.25 nmi), and debris flight to ground impact. Three burn scenarios were considered: nominal burn #4, 10% hot burn #4, and 10% cold and late burn #4. These scenarios were studied for both a prime, or "central pass" debris target zone, as well as a backup, or "western pass" zone. In addition to size and location results, island proximity was studied. These results showed that the Central Pass had no safety issues associated with it, and although the western pass did not satisfy land miss distance guidelines in NASA Safety Standard 1740.14, it was also seen that no debris should hit any land mass within a 3σ probability for either pass. All primary results are summarized in Table 14.

MODELING CHANGES SINCE CGRO

Since the successful deorbit and safe disposal of CGRO, the methods detailed herein have been continuously improved. These improvements include improved statistical handling of non-Gaussian output, leading to valid results for any number of Monte Carlo cases, with appropriate protection and confidence levels. Capabilities to model explosions during breakup, and breakup over an altitude range are also in the process of being added. The crossrange calculation is also being changed to be relative to the entry groundtrack, not the orbital groundtrack frozen at the initial state vector time.

Table 1: Intact (Reference) Mass and Aerodynamic Data, Intact CGRO Vehicle

Variable	Intact (Reference) Value
Mass	14010.0 kg (30886.7 lb)
Drag Coefficient	1.555
Aerodynamic Surface Area	46.0 m^2 (495.14 ft^2)
Ballistic Coefficient	195.8 kg/m^2 (40.1 psf)
L/D Ratio	0.0
Lift Coefficient	0.0

Table 2: Monte Carlo Mass and Aerodynamic Data, Intact CGRO Vehicle

Variable	Mean Value	Dispersion Limit (Uniform Distribution)
Mass	14010.0 kg (30886.7 lb)	36.6 kg (80.7 lb)
Drag Coefficient	1.555	0.645
Aerodynamic Surface Area	46.0 m^2 (495.14 ft^2)	0.0 m^2 (0.0 ft^2)
L/D Ratio	0.0	0.0

Table 3: Debris Ballistic Coefficient Ranges for Previous Disposal Analyses (ref. 6)

Entry Vehicle	Ballistic Coefficient Range
Space Shuttle External Tank	13.7 - 283.2 kg/m^2 (2.8 - 58 psf)
Apollo Service Module	2.4 - 463.8 kg/m^2 (0.5 - 95 psf)
Soyuz Service Module	6.8 - 566.4 kg/m^2 (1.4 - 116 psf)
Skylab	4.9 - 1562.4 kg/m^2 (1 - 320 psf)

Table 4: Monte Carlo Mass and Aerodynamic Data, General Debris

Variable	Mean Value	Dispersion Limit (Uniform Distribution)
Mass	22.7 kg (50.0 lb)	0.0 kg (0.0 lb)
Drag Coefficient	1.0	0.0
Aerodynamic Surface Area	4.66 m^2 (50.1852 ft^2)	4.63 m^2 (49.8148 ft^2)
L/D Ratio	0.075	0.075
Bank Angle	0.0 deg	180.0 deg

Table 5: Monte Carlo Mass and Aerodynamic Data, TASC Debris Only

Variable	Mean Value	Dispersion Limit (Uniform Distribution)
Mass	528.6 kg (1165.25 lb)	0.0 kg (0.0 lb)
Drag Coefficient	1.44	0.0
Aerodynamic Surface Area	0.30 m^2 (3.20685 ft^2)	0.01 m^2 (0.08255 ft^2)
L/D Ratio	0.075	0.075
Bank Angle	0.0 deg	180.0 deg

Table 6: Breakup Altitudes Found in Previous Disposal Analyses (ref. 6)

Entry Vehicle	Breakup Altitude
Space Shuttle External Tank (Actual Results)	61.1 - 83.3 km (33 - 45 nmi)
Space Shuttle Super Lightweight Tank (Assumed)	61.1 - 88.9 km (33 - 48 nmi)
Soyuz Service Module	64.8 - 83.3 km (35 - 45 nmi)
VAST/VASP	77.8 km (42 nmi)
Apollo Service Module	83.3 km (45 nmi)
Skylab	77.8 - 94.5 km (42 - 51 nmi)

Table 7: Reference Points for Range Values

Case	Center Pass	Western Pass
Geodetic Latitude	25.15° South	28.43° South
Longitude	70.46° West	71.21° West

Table 8: Nominal Burn 4 Monte Carlo Results, Center Pass

Statistic	Uprange from South America West Coast (km)	Crossrange from Orbit (km)
General Debris Footprint		
Maximum	9720.22	+80.40
Minimum	8227.70	-30.45
Average	9427.87	+24.72
Standard Deviation	222.80	19.56
Footprint Size	1336.77	117.32
TASC Footprint		
Maximum	8309.74	+71.01
Minimum	7365.03	-25.85
Average	7974.95	+21.84
Standard Deviation	172.24	18.21
Footprint Size	1033.42	109.29
Overall Footprint Geometric Center	8777.26 (4739.34 nmi)	+23.28 (12.57 nmi)
Overall Footprint Size	2638.01 (1424.41 nmi)	117.3 (63.35 nmi)

Table 9: 10% Hot Burn 4 Monte Carlo Results, Center Pass

Statistic	Uprange from South America West Coast (km)	Crossrange from Orbit (km)
General Debris Footprint		
Maximum	10406.39	+76.34
Minimum	9060.91	-33.21
Average	10132.83	+22.11
Standard Deviation	204.52	18.98
Footprint Size	1227.10	113.84
TASC Footprint		
Maximum	9132.55	+66.84
Minimum	8300.66	-26.54
Average	8842.56	+19.13
Standard Deviation	154.22	17.52
Footprint Size	925.30	105.08
Overall Footprint Geometric Center	9563.15 (5163.69 nmi)	+20.63 (11.14 nmi)
Overall Footprint Size	2366.47 (1277.79 nmi)	113.84 (61.47 nmi)

Table 10: 10% Cold/Late Burn 4 Monte Carlo Results, Center Pass

Statistic	**Uprange from South America West Coast (km)**	**Crossrange from Orbit (km)**
General Debris Footprint		
Maximum	7233.17	+70.14
Minimum	5278.76	-46.58
Average	6886.18	+12.74
Standard Deviation	272.32	20.65
Footprint Size	1633.91	123.94
TASC Footprint		
Maximum	5437.29	+60.50
Minimum	4079.40	-44.15
Average	4958.01	+8.72
Standard Deviation	231.02	19.59
Footprint Size	1386.11	117.58
Overall Footprint Geometric Center	5984.05 (3231.13 nmi)	+10.74 (5.80 nmi)
Overall Footprint Size	3438.18 (1856.47 nmi)	123.94 (66.92 nmi)

Table 11: Overall Monte Carlo Footprint Results for Center Pass

Statistic	**10% Hot Burn 4**	**Nominal Burn 4**	**10% Cold/Late Burn 4**
Crossrange Position of Geometric Center	+20.6 km (11.1 nmi)	+23.3 km (12.6 nmi)	+10.7 km (5.9 nmi)
Range Position of Geometric Center	9565 km (5165 nmi)	8780 km (4740 nmi)	5985 km (3230 nmi)
Length	2370 km (1280 nmi)	2640 km (1425 nmi)	3440 km (1855 nmi)
Width	114 km (61.5 nmi)	118 km (63.5 nmi)	124 km (66.9 nmi)
Overall Area to Protect:			
Crossrange Position of Geometric Center	15.6 km (8.4 nmi)		
Range Position of Geometric Center	7510 km (4055 nmi)		
Length	6480 km (3500 nmi)		
Width	135 km (72 nmi)		

Table 12: Overall Monte Carlo Derived Footprint Results for Western Pass

Statistic	**Overall Values**
Crossrange Position of Geometric Center	15.6 km (8.4 nmi)
Range Position of Geometric Center	9685 km (5230 nmi)
Length	6480 km (3500 nmi)
Width	135 km (72 nmi)

Table 13: 3σ Footprint Closest Approach Distances to Various Land Masses

Land Mass	**3σ Closest Approach Distance**
Center Pass	
West Coast of South America	4260 km (2300 nmi) uprange
Hawaii, United States	250 km (135 nmi) crossrange
Western Pass	
West Coast of South America	6465 km (3490 nmi) uprange
Palmyra Island, United States	119 km (64 nmi) crossrange
Washington Island, Kiribati	144 km (78 nmi) crossrange
Fanning Island, Kiribati	165 km (89 nmi) crossrange
Christmas Island, Kiribati	236 km (127 nmi) crossrange
Marquesas Islands, French Polynesia	252 km (136 nmi) crossrange

Table 14: Summary of GRO Debris Footprint Results

Statistic	**Nominal Burn Scenario**	**Covering all Burn Scenarios**
Length	2640 km (1425 nmi)	Monte Carlo: 6480 km (3500 nmi)
Width	118 km (63.5 nmi)	135 km (72 nmi)
Geometric Center Range from South America (in-plane)	Center Pass: 8780 km (4740 nmi) Western Pass: 10960 km (5915 nmi)	Center Pass: 7510 km (4055 nmi) Western Pass: 9685 km (5230 nmi)
Geometric Center Crossrange from Initial Orbit Groundtrack	23.3 km (12.6 nmi)	15.6 km (8.4 nmi)
Closest Approach to South America (uprange, 3σ)	Center Pass: 4260 km (2300 nmi) Western Pass: 6465 km (3490 nmi)	
Closest Approach to an Island (crossrange, 3σ)	Center Pass: 250 km (135 nmi) (Hawaii, United States) Western Pass: 119 km (64 nmi) (Palmyra, United States) 144 km (78 nmi) (Washington Island, Kiribati)	

Figure 1: Center Pass Nominal Burn 4 MC Extreme 3σ Impact Points - General Debris + TASC

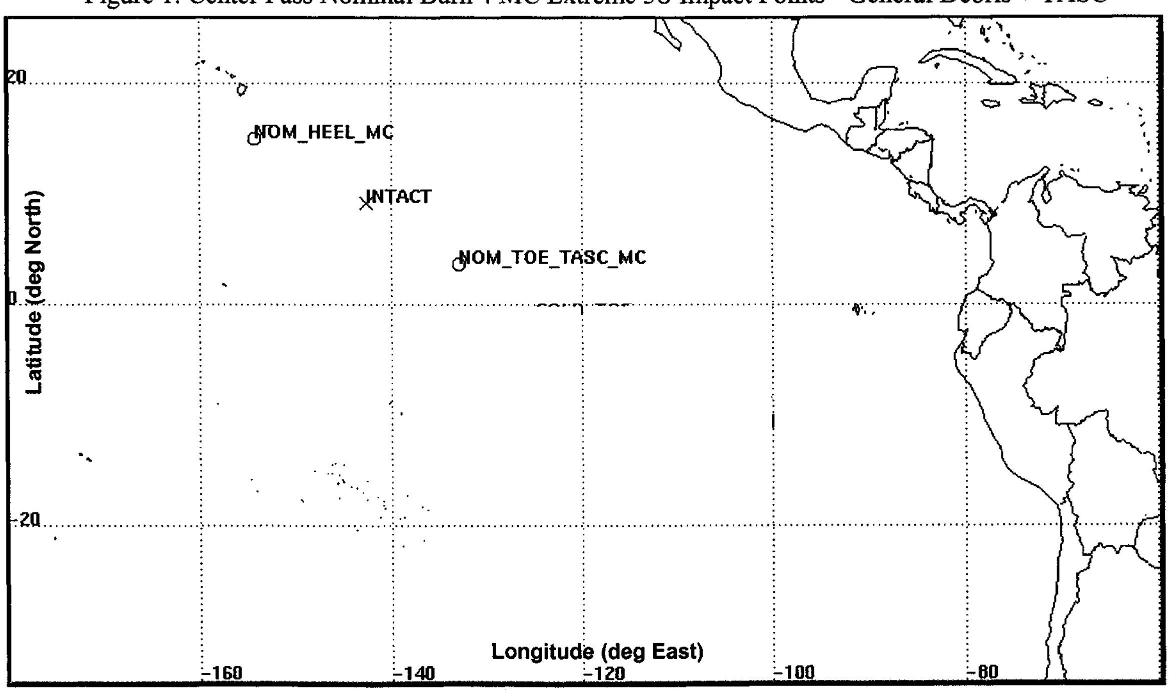

Figure 2: Center Pass 10% Hot Burn 4 Monte Carlo Extreme 3σ Impact Points - General Debris + TASC

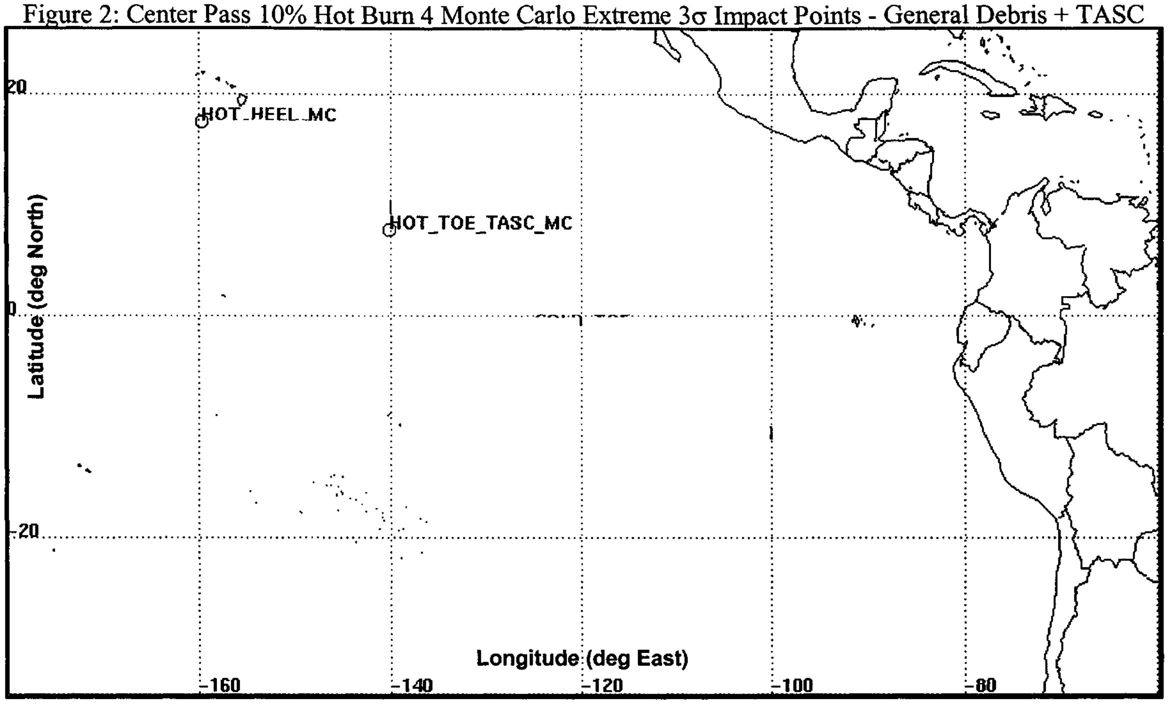

Figure 3: Center Pass 10% Cold/Late Burn 4 MC Extreme 3σ Impact Points - General Debris + TASC

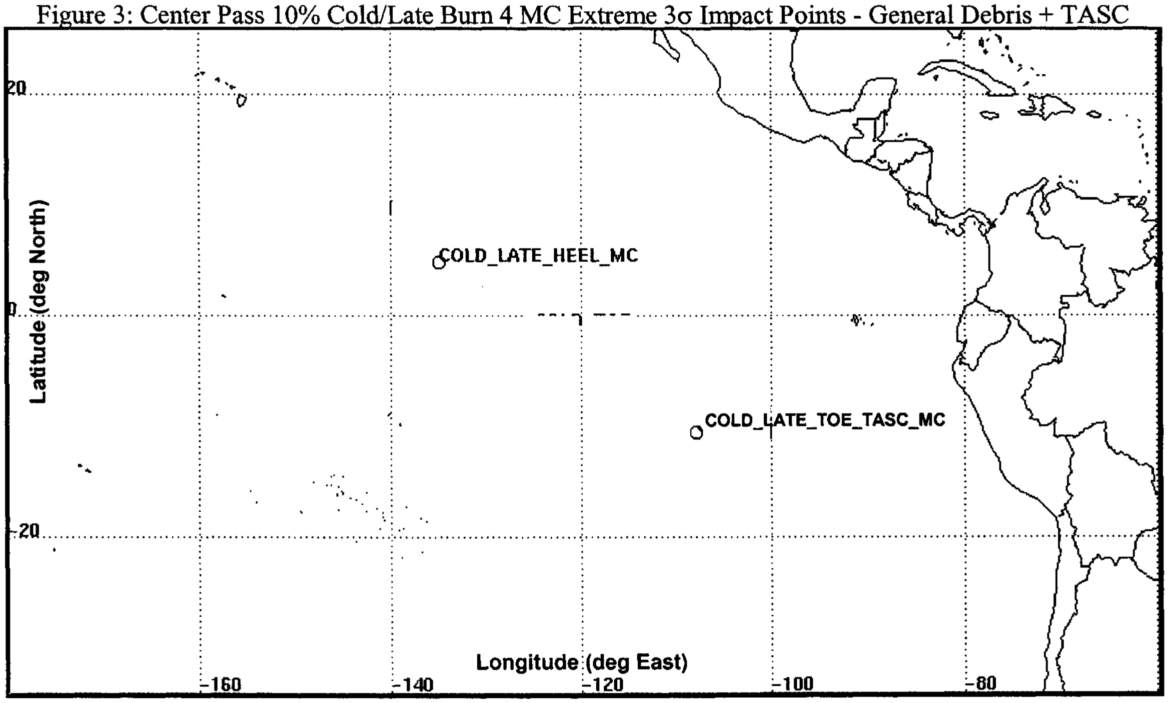

Figure 4: Footprint Length (General Debris) vs. Number of Monte Carlo Runs

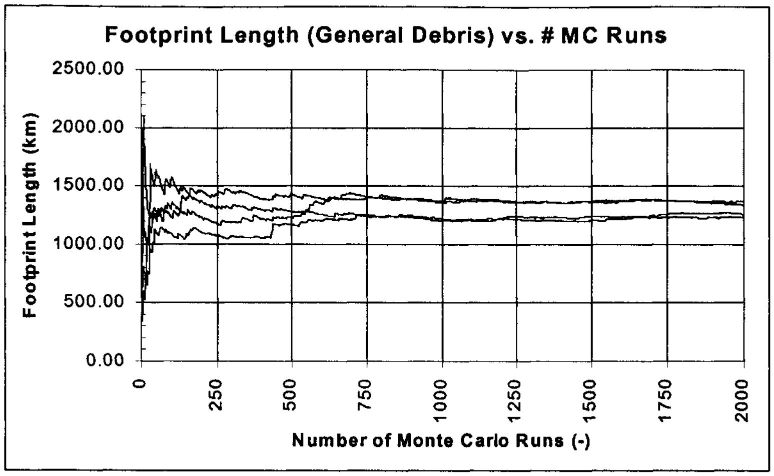

Figure 5: Footprint Width (General Debris) vs. Number of Monte Carlo Runs

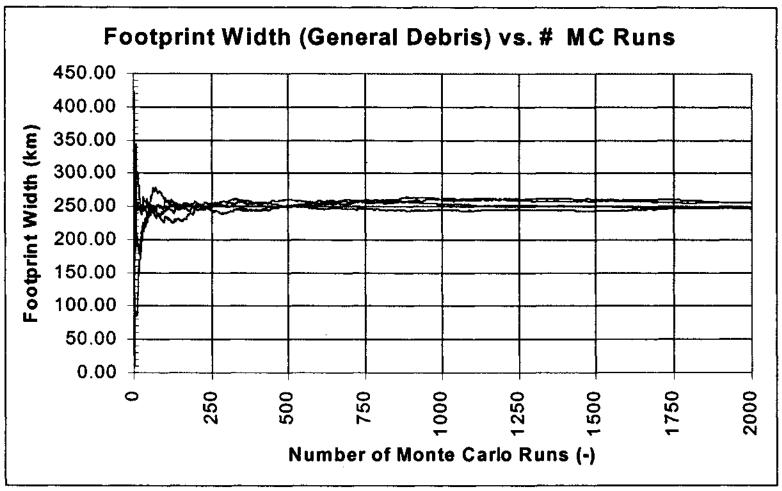

Figure 6: Footprint Center (General Debris) vs. Number of Monte Carlo Runs

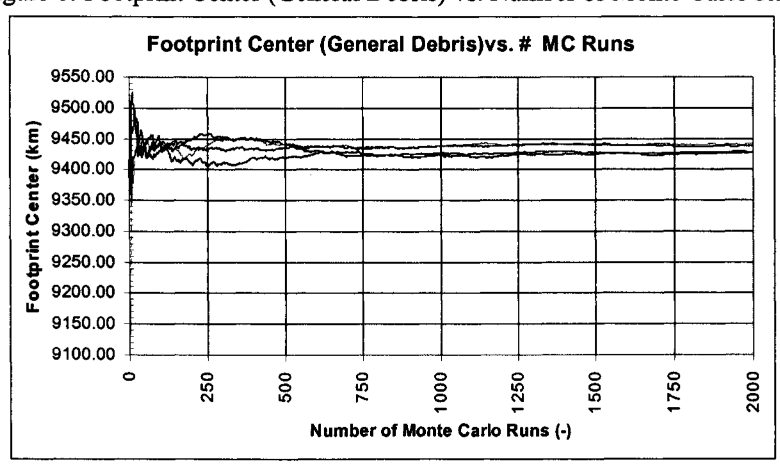

Figure 7: Center Pass Monte Carlo Extreme 3σ Impact Points, All Burns - General Debris + TASC

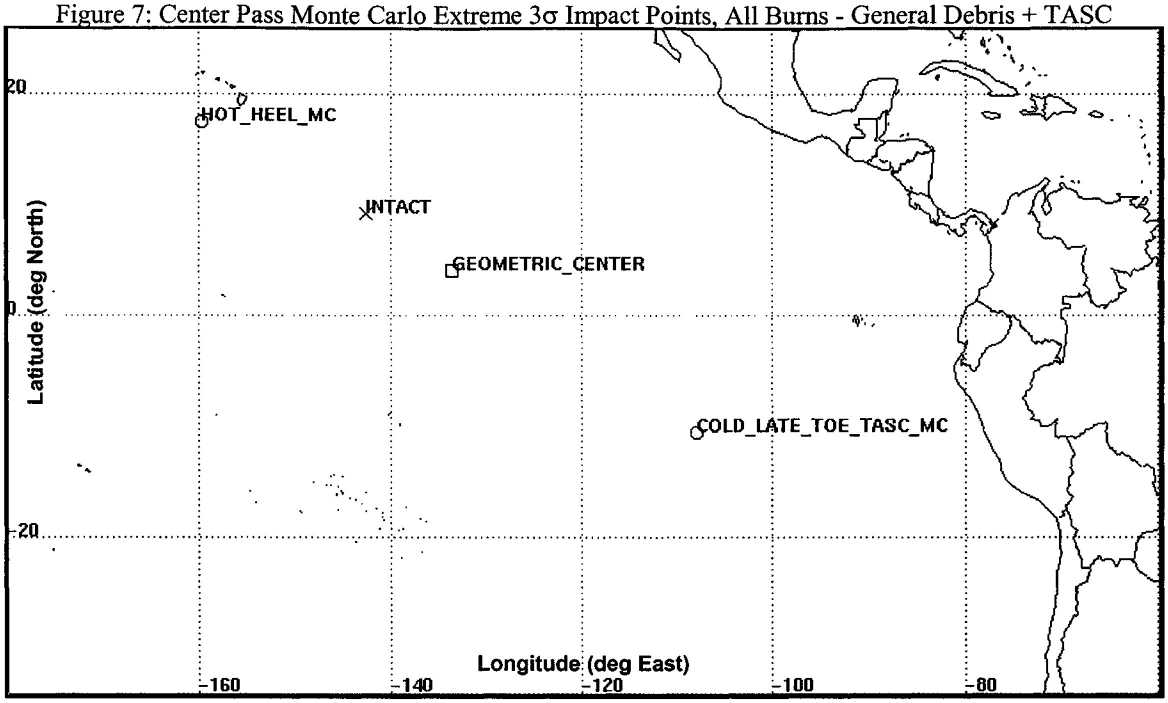

Figure 8: Derived Western Pass Monte Carlo Extreme 3σ Impact Points, All Burns - General Debris + TASC

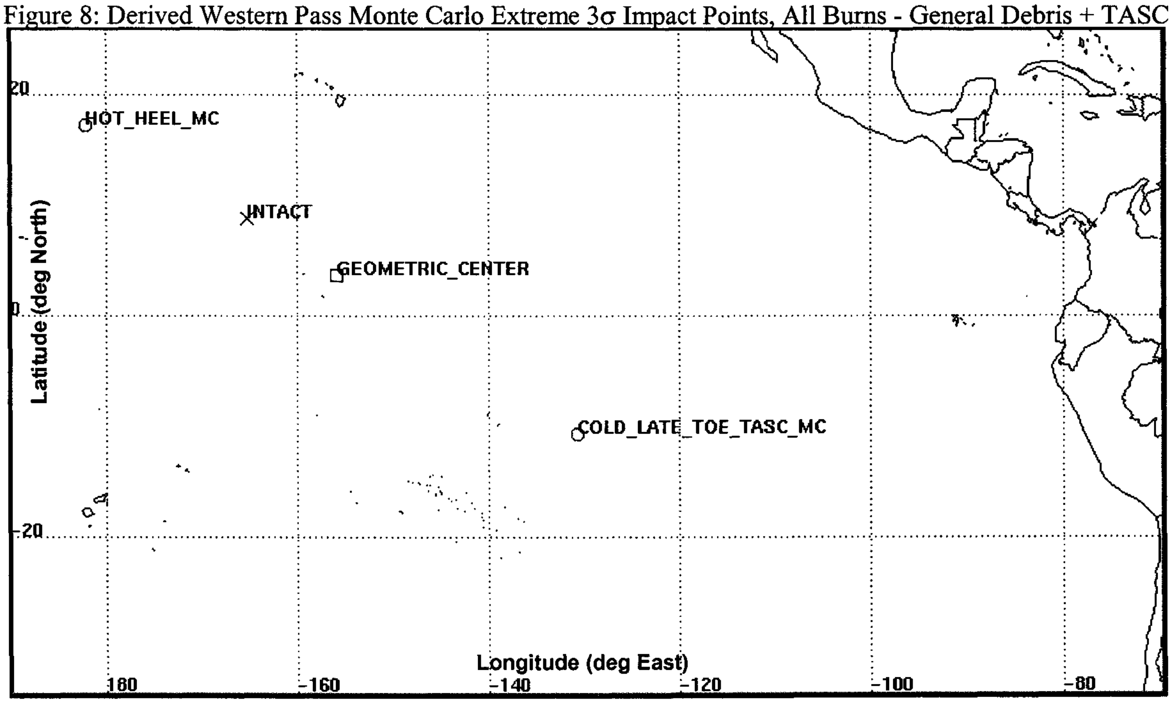

Figure 9: Footprint Proximity to Land Masses

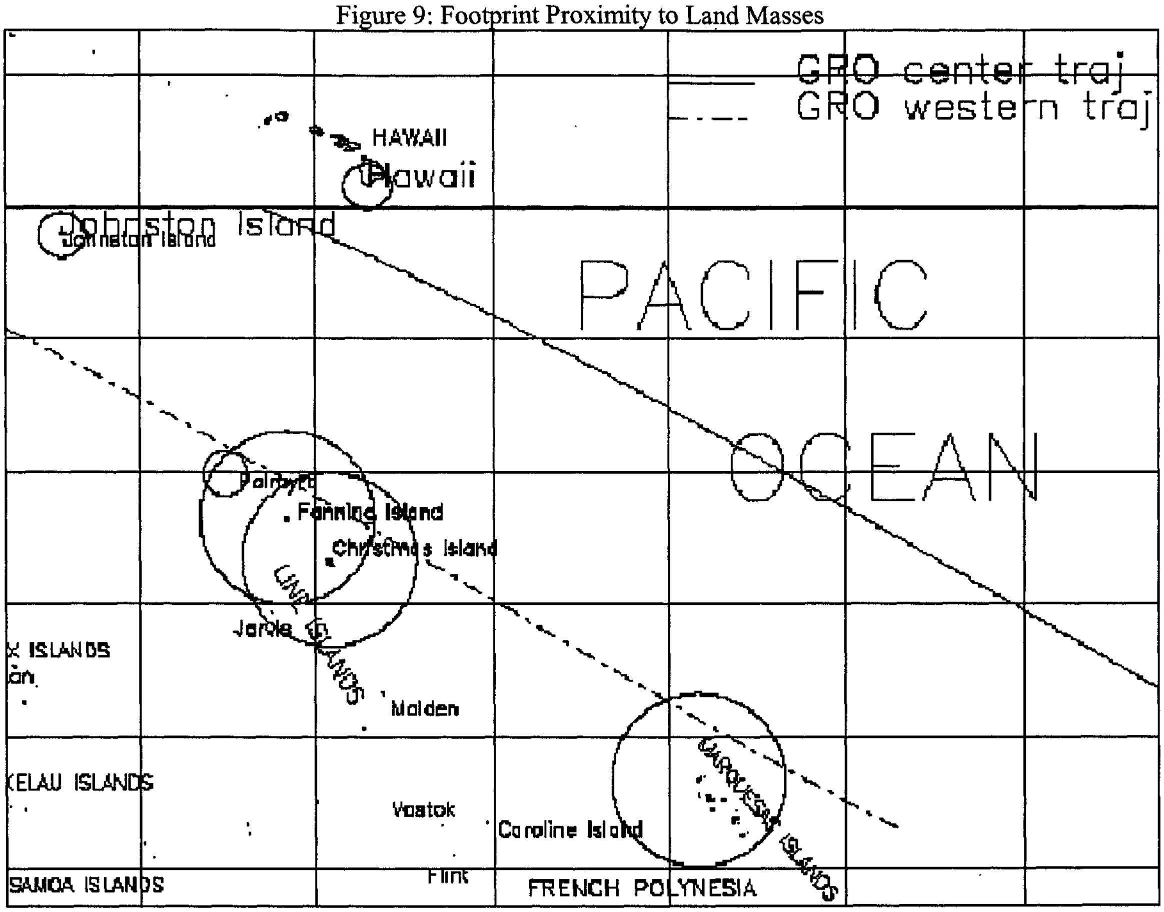

REFERENCES

1 Cole, C. E., "Gamma Ray Observatory Mission Contract, Observatory Reentry Plan (Final)," DRL 023, 40420-85-023-001, TRW Space & Technology Group, Federal Systems Division, July 31, 1985.

2 Brown-Conwell, E. R., "GRO Mission Flight Dynamics Analysis Report: Controlled Reentry of the Gamma Ray Observatory," CSC/TM-90/6001, Mission Report 90001, Flight Dynamics Division, NASA Goddard Space Flight Center, Greenbelt, Maryland, November 1989.

3 Berning, M. J., Sagis, K. D., "User's Guide for the Simulation and Optimization of Rocket Trajectories (SORT) Program, Version 7," NAS9-17900, Lockheed Engineering & Sciences Company, Houston, Texas, October, 1992.

4 Rao, P. P., Woeste, M. A., "Monte Carlo Analysis of Satellite Debris Footprint Dispersion," AIAA 79-1628, 1979.

5 Smith, R. N., Rochelle, W. C., "Reentry Survivability Analysis of Compton Gamma Ray Observatory (CGRO)," JSC-28929, Lockheed Martin Space Operations, NASA Johnson Space Center, Houston, Texas, March 2000.

6 Herdrich, R. J., and Nguyen, P. D., "Super Lightweight Tank (SLWT) Footprint Analysis: Technical Report," JSC-27712, NASA Johnson Space Center, Houston, Texas, March 01, 1997.

7 Refling, O., Stern, R., and Potz, C., "Review of Orbital Reentry Risk Predictions," Aerospace Report No. ATR-92(2835)-1, Programs Group, The Aerospace Corporation, El Segundo, California, July 15, 1992.

8 Gregory, F. D., "Guidelines and Assessment Procedures for Limiting Orbital Debris," NASA Safety Standard 1740.14, August 1995.